Bull. Mater. Sci., Vol. 38, No. 5, September 2015, pp. 1339–1344. © Indian Academy of Sciences.

Carbon nanotube-based coatings on titanium

ELZBIETA DLUGON[1], WOJCIECH SIMKA[2], ANETA FRACZEK-SZCZYPTA[1], WIKTOR NIEMIEC[1,*], JAROSLAW MARKOWSKI[3], MARZENA SZYMANSKA[4] and MARTA BLAZEWICZ[1]

[1]AGH University of Science and Technology, Faculty of Materials Science and Ceramics, Mickiewicza Avenue 30, 30-059 Krakow, Poland
[2]Silesian University of Technology, Faculty of Chemistry, B. Krzywoustego Street 6, 44-100 Gliwice, Poland
[3]Medical University of Silesia, Medykow Street 18, Bldg. C-1, 40-752 Katowice, Poland
[4]Lodz University of Technology, Faculty of Chemistry, Zeromskiego Street 116, 90-924 Lodz, Poland

MS received 21 March 2015; accepted 4 June 2015

Abstract. This paper reports results of the modification of titanium surface with multiwalled carbon nanotubes (CNTs). The Ti samples were covered with CNTs via electrophoretic deposition (EPD) process. Prior to EPD process, CNTs were functionalized by chemical treatment. Mechanical, electrochemical and biological properties of CNT-covered Ti samples were studied and compared to those obtained for unmodified titanium surface. Atomic force microscopy was used to investigate the surface topography. To determine micromechanical characteristics of CNT-covered metallic samples indentation tests were conducted. Throughout electrochemical studies were performed in order to characterize the impact of the coating on the corrosion of titanium substrate. *In vitro* experiments were conducted using the human osteoblast NHOst cell line. CNT layers shielded titanium from corrosion gave the surface-enhanced biointegrative properties. Cells proliferated better on the modified surface in comparison to unmodified titanium. The deposited layer enhanced cell adhesion and spreading as compared to titanium sample.

Keywords. CNT layers; surface modification; titanium surface; cell viability.

1. Introduction

Titanium and its alloys are commonly used as biomaterials for orthopaedic and dental implants.[1,2] These biomaterials possess a number of sought out properties like mechanical parameters suited for medical applications and higher than average resistance to corrosion. Despite that, their surface often needs to be modified in order to obtain proper osteointegrative properties. The most common method is the deposition of bioactive ceramic materials on the metal surface, which considerably improves the integration of titanium implant with bone tissue. There are a number of ways to obtain such layers including the plasma spray, sol–gel and hydrothermal methods.[3–7] Advancements in nanotechnology resulted in new ways for metallic surface modifications. Research shows that nanoengineered surfaces and anodized layers comprised of titanium oxide nanotubes, which have very good properties for medical applications.[8–10] The novel approach to metallic surface modification is the deposition of nanoparticle layer, including carbon nanoparticles–carbon nanotubes (CNTs). CNT displays unique biological properties that found increasing area of applications in the field of medical therapies and diagnostics, including tissue engineering, modern biosensors, implantable electrodes, as well as new materials for orthopaedic and dentistry implants.[11,12] In the field of tissue engineering, CNT can be used as a substrate for bone tissue mineralization. Coatings made of CNTs provide implants with enhanced bioactive properties and open new possibilities in terms of their biological functionalization.[13–15] They can also be further modified to increase the range of titanium biomedical applications.

In this paper, the results on the manufacture of multiwalled CNTs layer on titanium surface via electrophoretic deposition (EPD) process were reported.[16,17] Layer's mechanical, electrochemical and biological properties were investigated. The results were compared with those obtained for unmodified titanium surface.

2. Materials and methods

2.1 *CNTs*

In the experiments short CNTs were used (NanoAmor, width 1–2 μm, outer diameter 10–30 nm and inner diameter 5–10 nm). CNTs were purified and functionalized in a

*Author for correspondence (wniemiec@agh.edu.pl)

mixture of sulphuric (VI) acid and 65% nitric (V) acid with 3 : 1 ratio. The CNTs were immersed in acidic mixture at 70°C for 2 h. Subsequently, nanotubes were rinsed with distilled water and centrifuged. The CNT functionalization resulted in the creation of carboxylic (–COOH) and hydroxyl (–OH) groups on the surface of CNTs.

2.2 *EPD of CNT on titanium surface*

Functionalized CNTs dispersed in distilled water (5 mg in 10 cm^3) were deposited on both sides of titanium plates in the form of discs (10 mm diameter, 0.5 mm thick). Before deposition the plates were etched in 5% hydrofluoric acid for 30 s and rinsed abundantly with distilled water. The single plate served as an anode and was positioned between two negatively charged electrodes immersed in CNT suspension. Such set-up assured uniform coverage of both sides of the titanium plate with deposited CNTs. The static voltage of 28 V was applied for 30 s with current ranging from 6 to 13 mA. After the deposition, the specimens were dried for few minutes and put into exsiccator.

2.3 *Electrochemical analysis*

The corrosion resistance of pure titanium and CNT-covered titanium samples was investigated using Ringer's solution composed of 8.6 g dm^{-3} NaCl, 0.3 g dm^{-3} KCl, and 0.48 g dm^{-3} $CaCl_2 \cdot 6H_2O$ (Baxter, USA).[18–21] The apparatus consisted of a standard two-chamber electrolysis cell with three electrodes: a working electrode, a platinum auxiliary electrode and a Haber–Luggin capillary with a reference electrode (saturated calomel electrode – SCE). The electrolytic cell was powered by a potentiostat (PARSTAT 4000, AMETEK) equipped with Versa Studio software.

The investigations included the following measurements: (a) recording of the open circuit potential (E_{OCP}) as a function of time and (b) determining the $\log j = f(E)$ curve over a potential range (E_{OCP}) between –20 and +20 mV (dE/dt = 1 mV s^{-1}), which provides information regarding (1) the corrosion potential E_{CORR} (V); (2) the corrosion current density j_{CORR} (A cm^{-2}); (3) the polarization resistance R_p (kΩ cm^2); and (4) the cyclic polarization curve (CV) over a potential range (E_{OCP}) from –0.1 to 3 V (dE/dt = 10 mV s^{-1}). The corrosion characteristics such as a polarization resistance R_p, corrosion current density j_{CORR} and E_{CORR} were derived from potentiodynamic tests using the Stearn–Geary method. With this method corrosion current density can be determined if polarization resistance is known

$$j_{CORR} = ab/2.303(a + b)R_p = B/R_p,$$

where B is the Stern–Geary constant (V), a the slope of the anodic Tafel reaction (V/decade) and b the slope of the cathodic Tafel reaction (V/decade).

Polarization resistance was determined experimentally with equation

$$R_p = \Delta E/\Delta j.$$

2.4 *Micromechanical analysis*

Indentation tests on CNT-covered metallic samples were conducted using CSM Tester, instrument model MHTX S/N: 01-256. Diamond – Vickers – V-I 41 indenter was used. The load was set to 25 mN with the speed rate of 15% min^{-1}. The results were averaged from ten tests.

2.5 *Atomic force microscopy (AFM)*

AFM measurements were conducted in semicontact (tapping) mode using MultiMode 8 (Bruker) microscope using antimony-doped silicon tips with spring constant of 40 N m^{-1}.

2.6 *In vitro biological experiments*

In vitro experiments were conducted on CNT-covered titanium and pure titanium samples. The human osteoblast NHOst cell line (Lonza, Cat. no. CC-2538) was used. The cells were multiplied in MEM culture medium (PAA, Austria) with the addition of 10% foetal calf serum (PAA, Austria), 5% antibiotic solution, which included among others penicillin (UI cm^{-3}) and streptomycin (10 mg cm^{-3}), 100 mM sodium pyruvate solution, amino acids 100× non-essential solution (PAA, Austria). After rinsing the cultures with PBS and the addition of 5% trypsin with EDTA (PAA, Austria) the cell suspension was obtained. Trypsin was neutralized with the addition of medium. The cells were counted using Bürker chamber. The examined specimens and Thermanox glass culture slides (Nunc, USA) used as reference were placed in wells of cell culture multidish (Nunclon). As other reference sample the bottom of the multidish (polystyrene – PS) well was used. Briefly, 20,000 cells in suspension were added to every well. These were incubated in Galaxy 170s incubator (New Brunswick) in constant humidity in 5% carbon dioxide atmosphere at 37°C, for 3 and 7 days. For determination of cell viability ToxiLight_Bio Kit and ViaLight_Plus Kit test (LONZA Rockland Inc.) were used.

2.7 *Fluorescence microscopy*

Cell morphology on the titanium and CNT-covered titanium samples was investigated using inverted microscope Axiovert 40CFL with fluorescence add-on. The cells were dyed by immersion for 30 s in 100 µl of acridine orange followed by rinsing with PBS. This dye marks both living and dead cells with, respectively, green (with

the exception of lysosomes) and red (with the exception of nuclei) fluorescence. It happens due to degeneration of cell membrane in the cell fixation process, which enables the accumulation of the dye inside the cells. In addition, double-stranded RNA molecules are denaturized in this process. In case of live cells, the non-damaged membrane limits the amount of absorbed orange, which after bonding with RNA molecules emits green fluorescence.

3. Results and discussion

3.1 *Characterization of CNT layer on titanium surface*

The CNT layer deposited on the titanium surface via the EPD process exhibits fibrous mesh-like structure visible on atomic force microscopy (AFM) images (figure 1). Many nanotubes aggregate to form bundles. The layer's surface is uniform and shows isotropic morphology.

The results of electrochemical analysis of CNT layer on titanium surface and unmodified titanium specimen are shown in figure 2. The value of E_{OCP} of unmodified titanium specimen is rising, what is the effect of the creation of titanium oxide layer on the sample surface in Ringer's solution.[22] This potential for the titanium sample covered with CNT layer is shifted by *ca.* 0.5 V to anode side and it quickly stabilizes at 0.320 V. These results show that the titanium oxide layer on both samples has different electrical properties. It is most probably caused by integration of CNTs into oxide layer, as even modified CNTs have high electrical conductivity.[23]

Figure 3 shows the results of corrosion resistance analysis acquired by the linear polarization resistance (LPR)

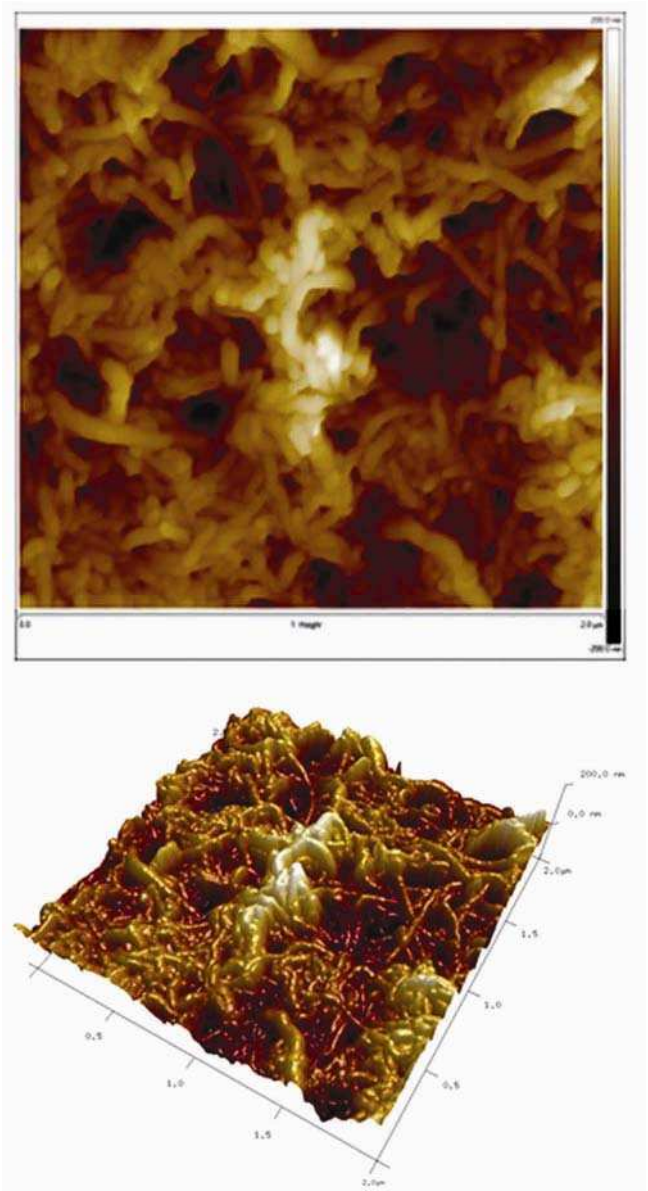

Figure 1. AFM image of CNT layer on titanium surface.

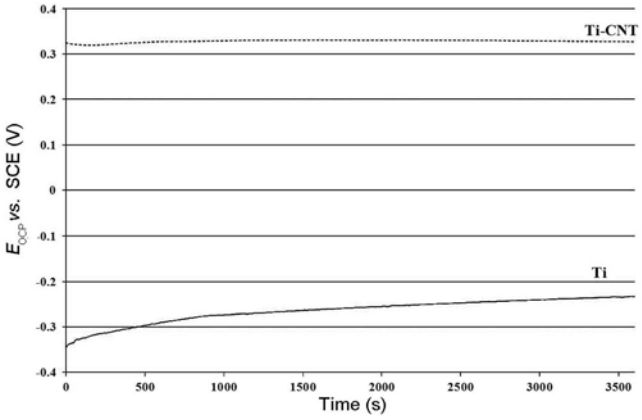

Figure 2. Variation of the E_{OCP} with time for the Ti and Ti-CNT samples in Ringer's solution.

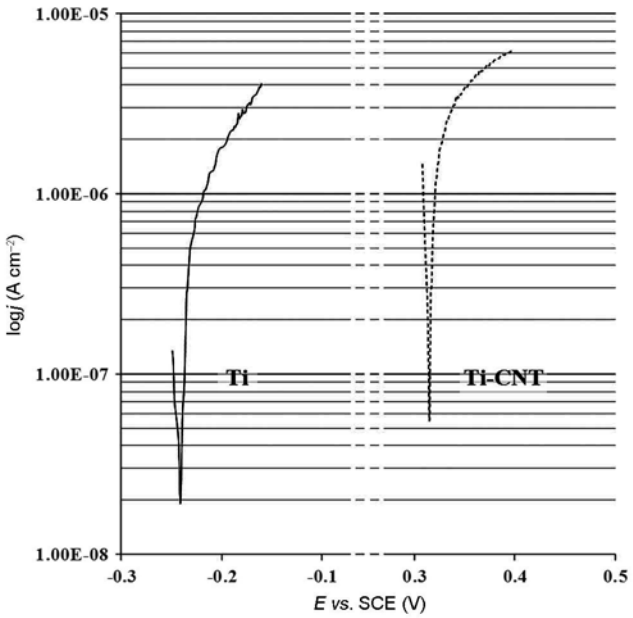

Figure 3. Polarization curves recorded for the Ti and Ti-CNT samples.

method. Corrosion potential (E_{CORR}), corrosion resistance (R_p) and corrosion current density (j_{CORR}) for both titanium and CNT-covered titanium can be found in table 1.

Based on these results the gradient composition of the surface of titanium modified in the EPD process can be proposed. The surface can be divided into two main parts – nanocomposite layer of CNT built into titanium oxide and surface-most layer of CNTs. It can be assumed that nanocomposite part is responsible for the shift in corrosion potential to positive values. The porous fibrous and conductive CNT layer on the surface contributes to noticeable decrease in corrosion resistance and increase in corrosion current density. The cyclic polarization curves showed in figure 4 strengthen this assumption as the curve acquired for titanium is typical,[24] while in case of modified titanium the rise of potential between 0.7 and 3 V is smooth and does not exhibit characteristic peaks. In the latter case, after reaching 3 V and change in the polarization, the current density dropped, although was still higher than in the case of pure titanium, what is coupled with the presence of the CNT layer on the titanium substrate. Generally, a lower corrosion resistance, R_p, or higher corrosion current, j_{CORR}, suggests high susceptibility to corrosion of investigated material. On the ground of corrosion experiments it could be concluded that the CNT-coated titanium is more prone to corrosion than unmodified titanium. However, the lower value of R_p and higher value of j_{CORR} are not related with corrosion processes of titanium sample but with the presence of thin, conductive, CNT network.[23] On the other hand the conductive CNT dispersed in TiO_2 layer (which is the cause of high corrosion currents) can act as a percolation pathways to a current flow.

3.2 *Mechanical analysis*

The results of indentation test of CNT layer on the titanium surface are shown in table 2. The table gathers values of h_{max} – the maximum indentation depth, HIT – indentation hardness, indentation modulus EIT and Vickers hardness of the nanocarbon layer. The values shown in the table are much lower than those obtained for the typical carbon and ceramic layers. However, analysis of the force–depth curve (figure 5) indicates that the layer hardness is depth-dependent. The outer layer displays a lower slope of load–depth curve, indicating its much higher susceptibility to be deformed as compared to the inner part of the layer. This can be caused by the EPD, as in the initial stages of the process the shorter and more functionalized nanotubes are deposited on the surface of titanium. This can lead to greater interactions and bonding between CNT. In addition the metal is anodized, thus this part of the layer is additionally reinforced by interactions of metal oxide with functionalized CNT. The subsequent nanotubes that reach the surface form interactions only with other CNT.

The indenter first pierces low-density CNT layer then reaches composite of CNT built into titanium oxide formed

Table 1. Linear polarization resistance experiment results: corrosion potential (E_{CORR}), corrosion resistance (R_p) and corrosion current density (j_{CORR}).

Sample	E_{CORR} (V)	R_p (kΩ cm^2)	j_{CORR} (A cm^{-2})
Ti	–0.239	60.7	20×10^{-8}
Ti-CNT	0.270	19.4	112×10^{-8}

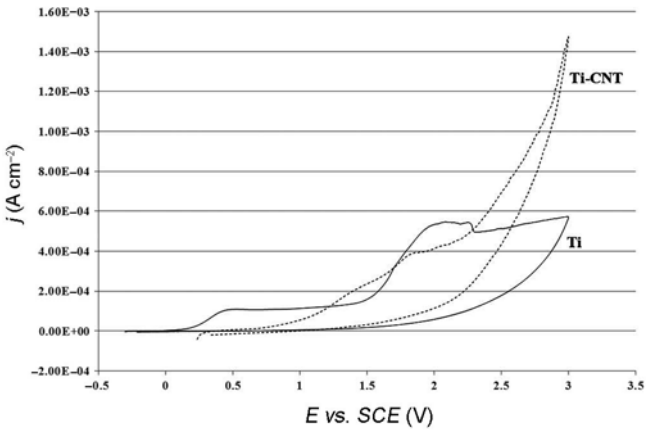

Figure 4. Cyclic voltammograms recorded for the Ti and Ti-CNT samples.

Table 2. Mechanical characteristics of CNT-covered Ti surface.

	10 mN			
Ti + CNT	h_{max} (nm)	HIT (MPa)	EIT (GPa)	HV
Mean	1965	1664	101	132
Standard deviation	± 271	± 107	± 15	± 37

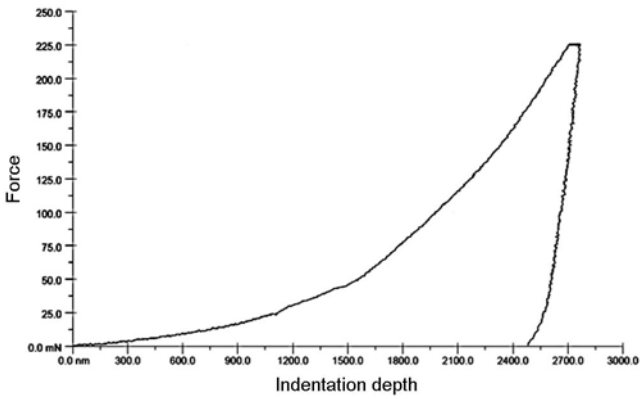

Figure 5. Loading–unloading curve for CNT-covered titanium in dependence from indentation depth.

in the EPD process. This results in a high toughness and low elastic modulus of the material.

CNT layer forms a gradient structure on the surface of the titanium with distinctly different properties than those of unmodified titanium. The surface-most part of the coating exhibits mechanical and electrical parameters as well as topography typical for CNT. Deeper in the layer the nanotubes create chemical bonds with titanium oxide formed directly on titanium surface, which results in strong bonding of the coating to the titanium surface.

3.3 *Biological analysis*

Figure 6 shows the diagram of cell viability in contact with samples after 3 and 7 days of incubation. After 3 days, the viability of cells on the titanium and CNT-modified surface is lower in comparison to the control. However, after 7 days culture cell viability on both samples is significantly enhanced compared to the third day of culture. The highest viability is obtained on the surface modified with CNT. This can be explained by the specific nanotopography of the surface, biomimetic shape of CNT as well as the presence of functional groups on their surface. This is in accordance with our previous studies which have shown high bioactivity of such nanotubes in contact with cells as well as in other bioactivity tests.[25,26] The results indicate that such modification of the biocompatible titanium surface significantly improves its biological properties and demonstrate the usefulness of such approach.

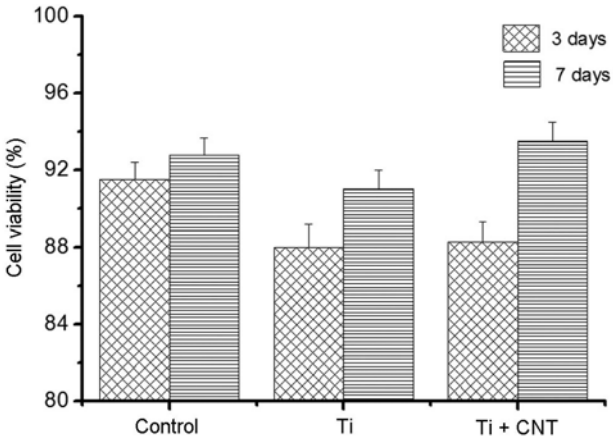

Figure 6. Viability of NHOst cells after 3 and 7 days culture on different surfaces. The data are expressed as mean ± SD from 8 to 11 measurements, Student's *t* test.

Figure 7 shows cell morphology on the surface of titanium and CNT-modified titanium after 7 days. The cells exhibit proper morphology. Both nucleus and cytoplasm are clearly visible in the images. The cells uniformly cover the surface of the samples. On the titanium sample (figure 7A) cells display fibrous shape, while on CNT coating (figure 7B) the cell shape is more flattened, which suggests their better adhesion to that surface, which confirms that the carbon layer promotes adhesion of bone cells.

4. Conclusions

With the use of EPD process, the surface of the titanium can be coated with thin layer of functionalized CNTs. The process is both quick and simple. The acquired coating shields titanium from corrosion as well as gives the

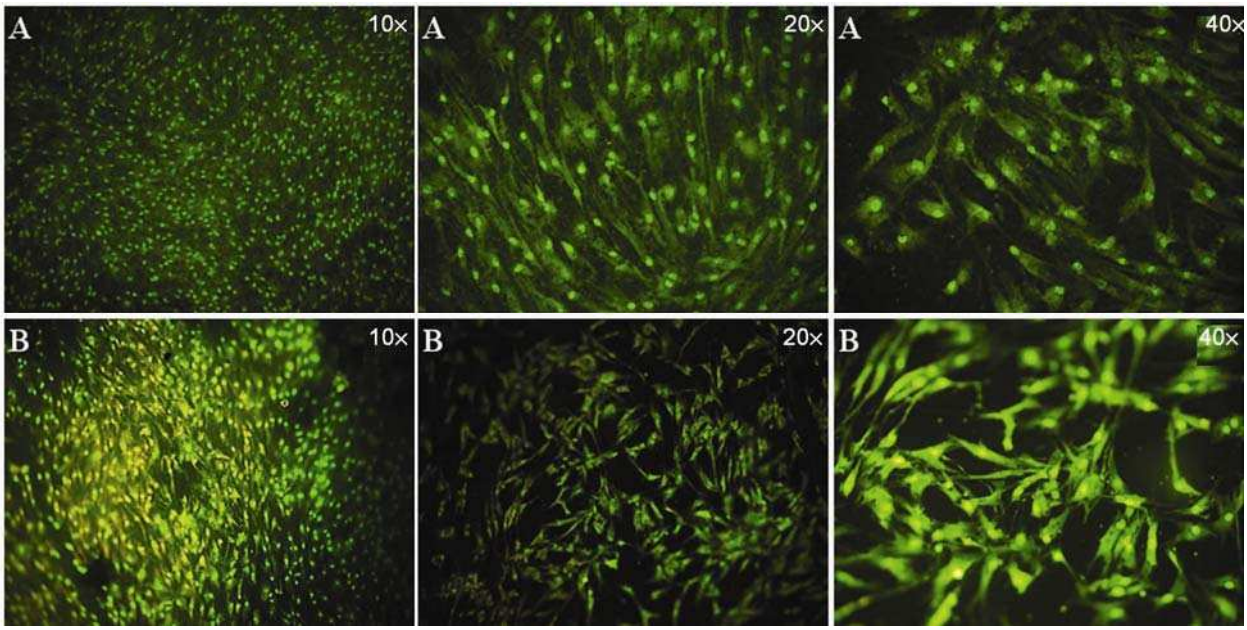

Figure 7. NHOst cell morphology stained with acridine orange on Ti surface (**A**) and CNT-covered Ti surface (**B**) after 7 days of culture (mag. 10×, 20× and 40×).

surface-enhanced osteointegrative properties. Cells proliferate better on modified surface in comparison to unmodified titanium. This can have a positive effect on implant–tissue interface adhesive strength, which is a key feature for metal-based implants. As such this new composite coating is a very promising modification for dental and load-bearing implants.

Acknowledgement

This work has been supported by the NCN (National Science Centre – Poland) Grant: UMO-2011/01/B/ST5/06424.

References

1. Niinomi M 2008 *Mater. Trans.* **49** 2170
2. Rack H J and Quazi J I 2006 *Mater. Sci. Eng. C* **26** 1269
3. Xuanyong L, Chu P K and Ding C 2004 *Mater. Sci. Eng. R: Rep.* **47** 49
4. Duran A, Conde A, Gomez C A, Dorado T, Garcıa C and Cere S 2004 *J. Mater. Chem.* **14** 2282
5. Lu Y P, Li M S, Li S T, Wang Z G and Zhu R F 2004 *Biomaterials* **25** 4393
6. Man H C, Chiu K Y, Cheng F T and Wong K H 2009 *Thin Solid Films* **517** 96
7. Rajesh P, Muraleedharan C V, Komath M and Verma H 2011 *J. Mater. Sci.: Mater. Med.* **22** 497
8. Wall I, Donos N, Carlqvist K, Jones F and Brett P 2009 *Bone* **45** 17
9. Larsson Wexell C, Thomsen P, Aronsson B, Tengvall P, Rodahl M, Lausmaa J, Kasemo B and Ericson L E 2013 *Int. J. Biomater.* Article ID 412482
10. Vindigni V, Stellini E, Gardin C, Ferroni L, Sivolella S and Zavan B 2013 *Int. J. Mol. Sci.* **14** 1918
11. Zhang Y, Bai Y and Yan B 2010 *Drug Discov. Today* **15** 428
12. Liao H, Paratala B, Sitharaman B and Wang Y 2011 *Methods Mol. Biol.* **726** 223
13. Cho J, Konopka K, Rozniatowski K, García-Lecinac E, Shafferd M S P and Boccaccini A R 2009 *Carbon* **47** 58
14. Fraczek-Szczypta A, Długon E, Weselucha-Birczynska A, Nocun M and Blazewicz M 2013 *J. Mol. Struct.* **1040** 238
15. Li X, Liu X, Huang J, Fan Y and Cui F 2011 *Surf. Coat. Technol.* **206** 759
16. Besra L and Liu M 2007 *Prog. Mater. Sci.* **52** 1
17. Raddaha N S, Cordero-Arias K, Cabanas-Polo S, Virtanen S, Roether J A and Boccaccini A R 2014 *Materials* **7** 1814
18. Assis S L, Wolynec S and Costa I 2006 *Electrochim. Acta* **51** 1815
19. Oliveira N T C, Ferreira E A, Duarte L T, Biaggio S R, Rocha-Filho R C and Bocchi N 2006 *Electrochim. Acta* **51** 2068
20. Robin A, Carvalho O A S, Schneider S G and Schneider S 2008 *Mater. Corros.* **59** 929
21. Souto M R, Laz M M and Reis R L 2003 *Biomaterials* **24** 4213
22. Szewczenko J, Nowinska K and Marciniak J 2011 *Przegląd Elektrotech./Electrotech. Rev*. **87** 228
23. Lima M D, de Andrade M J, Bergmann C P and Roth S 2008 *J. Mater. Chem.* **18** 776
24. Simka W, Sadkowski A, Warczak M, Iwaniak A, Dercz G, Michalska J and Maciej A 2011 *Electrochim. Acta* **56** 8962
25. Benko A, Przekora A, Nocuń M, Wesełucha-Birczyńska A, Ginalska G and Błażewicz M 2014 *Eng. Biomater.* **128–129** 93
26. Długon E, Niemiec W, Fraczek-Szczypta A, Jelen P, Sitarz M and Blazewicz M 2014 *Spectrochim. Acta A* **133** 872